The Characteristics of Pulverized Coal Combustion in the Two Stage Cyclone Combustor

Nahm Roh Joo
Graduate School, Department of Mechanical Engineering, Korea University 1, 5-ka, Anam-dong, Sungbuk-ku, Seoul 136-701, Korea
Ho Young Kim*, Jin Taek Chung
Department of Mechanical Engineering, Korea University 1, 5-ka, Anam-dong, Sungbuk-ku, Seoul 136-701, Korea
Sang Il Choi
Low Emission Combustion Research Team, Korea Institute of Energy Research 71-2, Jang-dong, Yusung-ku, Daejon 305-343, Korea

Numerical investigations on air staging and fuel staging were carried out with a newly designed coaxial cyclone combustor, which uses the method of two stage coal combustion composed of pre-combustor and main combustor. The pre-combustor with a high air/fuel ratio is designed to supply gas at high temperature to the main combustor. To avoid local high temperature region in this process, secondary air is injected in the downstream. Together with the burned gas supplied from the pre-combustor and the preheated air directly injected into main combustor, coals supplied through the main burner react rapidly at a low air/fuel ratio. Strong swirling motion of cyclone combustor keeps the wall temperature high, which makes slagging combustion possible. Alaska, US coal is used for calculations. Predictions were made for various coal flow rates in the main combustor for fuel staging and for the various flow rate of secondary air in the pre-combustor for air staging. In-scattering angles are also chosen as a variable to increase residence times of coal particles. Temperature fields and particle trajectories for various conditions are described. Predicted temperature variations at the wall of the combustor are compared with corresponding experimental data and show a similar trend. The in-scattering angle of 20° is recommended to increase the combustion efficiency in the main chamber.

Key Words : Pulverized Cool, Fuel Staging, Air Staging, Two-stage Cyclone Combustor

1. Introduction

In pulverized coal power plants, it is necessary to control environmental pollutants, such as NOx, unburned carbon and fly ash. In order to reduce NOx formations, air staging and fuel staging methods are applied effectively. Air staging divides the combustion process into a primary zone run with a deficiency of air and a secondary burnout zone run with an excess air. The formation of NOx decreases at low stoichiometric air/fuel ratio and then additional air is supplied for the complete burnout of coal particles. In fuel staging, the reducing conditions are created only subsequent to a combustion zone by adding a reburning fuel. Gaseous fuels with a good combustibility are generally used for reburning.

* Corresponding Author,
E-mail : kimhy@korea.ac.kr
TEL : +82-2-3290-3356; **FAX** : +82-2-926-9290
Department of Mechanical Engineering, Korea University 1, 5-ka, Anam-dong, Sungbuk-ku, Seoul 136-701 Korea. (Manuscript **Received** June 25, 2001; **Revised** June 10, 2002)

In a modern industrial furnace, a combination of both staging is mostly used (Spliethoff et al., 1996 ; Kimoto et al., 1995).

In order to reduce the amount of unburned carbon and make the slagging combustion possible, cyclone combustors are often used. A typical burner configuration for pulverized coal combustion in cylindrical furnaces consists of two coaxial air streams, the inner one of which carries the pulverized fuel (Abbas et al., 1997 ; Anagnostopoulos et al., 1993 ; Weber et al., 1992 ; Visser et al., 1990 ; Lockwood et al., 1988 ; Jamaluddin et al., 1987 ; Nikjooy et al., 1988 ; Lockwood et al., 1984 ; Truelove, 1984). But in a cyclone combustor, the tangential air injection causes a swirling motion in the combustor and coal particles show spiral trajectories especially in the vicinity of the wall. Therefore, the wall temperature is kept high, which allows the slagging condition at the wall.

Objective of the present study is to predict the combustion characteristics in a coaxial 2-stage cyclone combustor, which was newly designed. Investigation into various modes of air staging and fuel staging, for burning pulverized coal, was carried out with a bench-scale coal combustor. Various flow rate of coal in the main combustor and flow rate of the secondary air in the pre-combustor are considered. Temperature fields, particle trajectories and residence times are predicted for various in-scattering angles.

2. Theoretical Models

The numerical calculation of the two-phase turbulent reacting flow is based on the so-called particle-source-in-cell (PSIC) method, in which the gas and particle phases are treated by the Eulerian and Lagrangian approaches, respectively.

2.1 Gas phase equations

The general conservation equations of the axisymmetric turbulent gas flow field can be written for a variable ϕ as follows :

$$\frac{\partial}{\partial x}(\rho u\phi)+\frac{1}{r}\frac{\partial}{\partial r}(r\rho v\phi) =\frac{\partial}{\partial x}\left(\Gamma_\phi\frac{\partial\phi}{\partial x}\right)+\frac{1}{r}\frac{\partial}{\partial r}\left(r\Gamma_\phi\frac{\partial\phi}{\partial r}\right)+S_\phi+S_{p\phi} \quad (1)$$

The source terms of the gas phase, S_ϕ, the particle phase, $S_{p\phi}$, and the exchange coefficient, Γ_ϕ, are summarized in Table 1. The time-averaged transport equations for mass, momentum, turbulence kinetic energy and its dissipation rate, enthalpy and mixture fraction are solved numerically. The popular $k-\varepsilon$ turbulence model is known to be deficient for swirling flows due to the neglect of anisotropy, especially in the case of combustion (Shim et al., 1994). Because of the comparatively strong swirling motion in a cyclone combustor, the Reynolds Stress Model for turbulence calculation is used in this study. P-1 model is used for the thermal radiation transfer, which is expressed in the form of transport equation.

2.2 Particle phase equations

2.2.1 Equations of Motion

The coal particle is tracked by solving the Lagrangian equations of motion with a stochastic treatment for particle dispersion. Particles are divided into a number of groups with the same properties such as position, velocity and diameter at the inlet port. The k th computational particle has the number flow rate of n_k. Reduced differential equations for the particle velocity $\vec{u}_{pi}$ and the position x_{pi} can be written as follows :

$$\frac{d\vec{u}_{pi}}{dt}=\left(\frac{3C_D\mu\mathrm{Re}}{4\rho_p{d_p}^2}\right)(\vec{u}_i-\vec{u}_{pi}) \quad (2)$$

$$\frac{dx_{pi}}{dt}=\vec{u}_{pi} \quad (3)$$

where $\vec{u}_i$ is the instantaneous gas phase velocity defined as the summation of mean and fluctuating components, C_D is the drag coefficient and Re is the particle Reynolds number defined by

$$\mathrm{Re}=\rho d_p\,|\,\vec{u}_i-\vec{u}_{pi}\,|/\mu \quad (4)$$

2.2.2 Coal Devolatilization

The coal devolatilization is approximated by a first-order single reaction model with the form given by :

$$\frac{dm_p}{dt}=-k(m_p-(1-f_{v0})\,m_{p0}) \quad (5)$$

Table 1 Definition of diffusion coefficients and source terms

Equation	ϕ	Γ	S_ϕ	$S_{p\phi}$
Continuity	1	0	0	$\frac{1}{\mathrm{Vol}}\sum n_k\left(\frac{dm_p}{dt}\right)_k$
Axial Momentum	u	μ_e	$-\frac{\partial p}{\partial x}+\frac{\partial}{\partial x}\left(\mu\frac{\partial u}{\partial x}\right)+\frac{1}{r}\frac{\partial}{\partial r}\left(r\mu\frac{\partial v}{\partial x}\right)$ $-\frac{\partial}{\partial x}(\rho\overline{u'u'})-\frac{\partial}{\partial r}(\rho\overline{u'v'})$	$\frac{1}{\mathrm{Vol}}\sum n_k\left(\frac{dm_pu_p}{dt}\right)_k$
Radial Momentum	v	μ_e	$-\frac{\partial p}{\partial r}+\frac{\partial}{\partial x}\left(\mu\frac{\partial u}{\partial r}\right)+\frac{1}{r}\frac{\partial}{\partial r}\left(r\mu\frac{\partial v}{\partial r}\right)-2\mu\frac{v}{r^2}+\rho\frac{w^2}{r}$ $-\frac{\partial}{\partial x}(\partial\overline{v'u'})-\frac{\partial}{\partial r}(\partial\overline{v'v'})$	$\frac{1}{\mathrm{Vol}}\sum n_k\left(\frac{dm_pv_p}{dt}\right)_k$
Tangential Momentum	w	μ_e	$-\rho\frac{vw}{r}-\frac{w}{r^2}\frac{\partial r\mu}{\partial r}-\frac{\partial}{\partial x}(\rho\overline{w'u'})-\frac{\partial}{\partial r}(\rho\overline{w'v'})$	$\frac{1}{\mathrm{Vol}}\sum n_k\left(\frac{dm_pw_p}{dt}\right)_k$
Reynolds Stress	$\overline{u_i'u_j'}$	$\frac{\mu_e}{\sigma_k}$	$P_{ij}+\Phi_{ij}-\frac{2}{3}\varepsilon\delta_{ij}$	0
Dissipation Rate	ε	$\frac{\mu_e}{\sigma_\varepsilon}$	$\frac{\varepsilon}{k}(C_{\varepsilon1}G_k-C_{\varepsilon2}\rho\varepsilon)$	0
Mixture Fraction	f	$\frac{\mu_e}{\sigma_f}$	0	$\frac{1}{\mathrm{Vol}}\sum n_k\left(\frac{dm_p}{dt}\right)_k$
Variance	g	$\frac{\mu_e}{\sigma_g}$	$C_{g1}\mu_t\left[\left(\frac{\partial f}{\partial x}\right)^2+\left(\frac{\partial f}{\partial r}\right)^2\right]-C_{g2}\rho\frac{\varepsilon}{k}g$	0
Enthalpy	h	$\frac{\mu_e}{\sigma_h}$	$Q_{\mathrm{radiation}}$	$\frac{1}{\mathrm{Vol}}\sum n_k\left(\frac{dm_ph_p}{dt}\right)_k$

$$P_{ij}=-\left(\overline{u_i'u_k'}\frac{\partial u_j}{\partial x_k}+\overline{u_j'u_k'}\frac{\partial u_i}{\partial x_k}\right)$$

$$\Phi_{ij}=-C_3\frac{\varepsilon}{k}\left(\overline{u_i'u_j'}-\frac{2}{3}k\delta_{ij}\right)-C_4\left(P_{ij}-\frac{2}{3}G_k\delta_{ij}\right)$$

$$G_k=\mu_t\left[2\left\{\left(\frac{\partial u}{\partial x}\right)^2+\left(\frac{\partial v}{\partial r}\right)^2+\left(\frac{v}{r}\right)^2\right\}+\left(\frac{\partial u}{\partial r}+\frac{\partial v}{\partial x}\right)^2+\left(\frac{\partial w}{\partial x}\right)^2+\left(r\frac{\partial}{\partial r}\left(\frac{w}{r}\right)\right)^2\right]$$

$C_{\varepsilon1}=1.44$, $C_{\varepsilon2}=1.92$, $C_{g1}=2.86$, $C_{g2}=2.0$, $\sigma_k=1.0$, $\sigma_\varepsilon=1.3$, $\sigma_f=0.7$, $\sigma_g=0.7$, $\sigma_h=0.7$, $C_3=1.8$, $C_4=0.6$

where m_p is the particle mass, m_{p0} is the initial particle mass, f_{v0} is the fraction of volatiles and k is the rate constant of Arrhenius expression such as:

$$k_v=A_v\exp(-E_v/RT_p) \tag{6}$$

The kinetic parameters ($A_v=8.36\times10^4 s^{-1}$, $E_v=7.4\times10^7$ J/kg·mol) recommended by Badzioch et al. (1970) are used.

The particle diameter also varies in the process of devolatilization according to the swelling coefficient, C_{sw}, as follows:

$$\frac{d_p}{d_{p0}}=1+(C_{sw}-1)\frac{m_{p0}-m_p}{f_{v0}m_{p0}} \tag{7}$$

where f_{v0} and m_{p0} indicate initial volatile fraction and initial mass of particle, respectively.

Heat balance for a particle during the devolatilization process is calculated as follows:

$$m_pC_{Pp}\frac{dT_p}{dt}=hA_p(T_\infty-T_p)+\frac{dm_p}{dt}Q_L+\varepsilon_pA_p\sigma(\theta_R^4-T_p^4) \tag{8}$$

where C_{Pp} is the heat capacity of the particle (J/kg·K), h is the convective heat transfer coefficient (W/m²·K), Q_L is the latent heat (J/kg), ε_p is the particle emissivity, σ is the Boltzmann's constant (5.67×10^{-8} W/m²·K⁴) and θ_R is the radiative temperature ($\theta_R^4=I/4\sigma$).

2.2.3 Char combustion

The reaction between char (taken to be pure carbon) and oxygen at the surface of the particle is assumed to produce carbon monoxide which is

subsequently oxidized to carbon dioxide in the gas phase. The char combustion is controlled by the oxygen diffusion rate to the particle surface (k_d) as well as the kinetic reaction rate (k_c). In addition, the overall rate of reaction is expressed by their harmonic mean as follows (Field, 1969; Baum & Street, 1971):

$$k_t=\frac{1}{1/k_d+1/k_c} \tag{9}$$

where the diffusion rate can be given by

$$k_d=C_1\frac{[(T_p+T_\infty)/2]^{0.75}}{d_p} \tag{10}$$

and the kinetic reaction rate is expressed in the Arrhenius form as

$$k_c=A_c\exp(-E_c/RT_p) \tag{11}$$

where A_c and E_c are the preexponential factor ($=0.03s^{-1}$) and the apparent activation energy ($=9.2\times10^7$ J/kg·mol), respectively.

The change of particle temperature during char combustion is calculated from

$$m_pC_{Pp}\frac{dT_p}{dt}=hA_p(T_\infty-T_p)-f_h\frac{dm_p}{dt}H+\varepsilon_pA_p\sigma(\theta_R^4-T_p^4) \tag{12}$$

where H is the heat of reaction (J/kg). The particle absorbs a fraction (f_h) of the energy produced by the char burnout and the rest is supplied to the gas phase.

2.3 Combustion model

Chemical reactions in the gas phase are assumed to occur rapidly and are limited by the mixing rates of fuel and oxidant so that the well-known mixture fraction approach can be applied and gaseous fuel atoms are algebraically related to the mixture fraction. Therefore, species concentrations are predicted from mixture fraction and the variance of mixture fraction fluctuations. Combustion of the devolatilized fuel from coal particle is modeled by β-probability density function (PDF) model with chemical equilibrium. In order to account for the heat exchange between gas and particle phases, a three-dimensional look-up table is generated, where the properties depend on not only mean and variance of mixture fraction but also the enthalpy level.

3. Computational Details

Figure 1 shows the coaxial 2-stage cyclone combustor with inlet ports. The pre-combustor, in which stoichiometric air/fuel ratio is as low as 0.55, is designed to supply gas at high temperature to the main combustor. To avoid local high temperature region in this process, the secondary air is injected through inlet 3, which is known as air staging. Together with the burned gas supplied from the pre-combustor and the preheated air directly injected into main combustor through inlet 4, coals supplied through inlet 1 burn rapidly at a low stoichiometric air/fuel ratio, which is known as fuel staging.

Coals are supplied axially through inlet 1 and tangentially through inlet 2 with primary air at atmospheric temperature. Coal particles are pulverized so that the fraction of coals smaller than 74 μm is 70 % and measured mean diameter

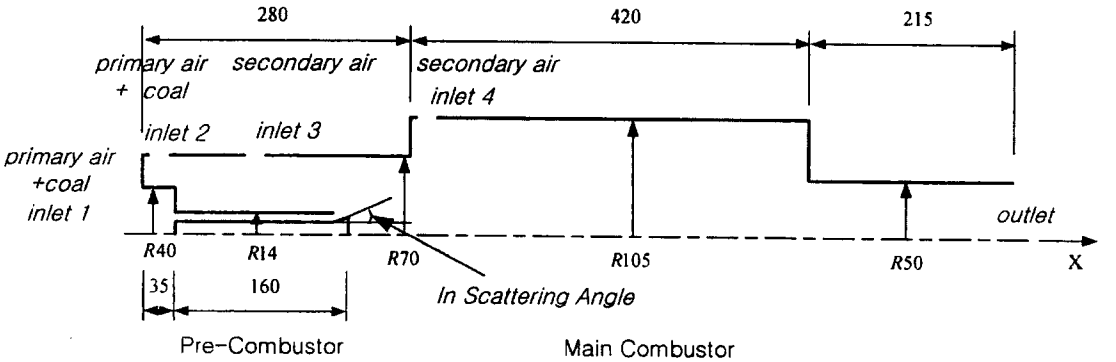

Fig. 1 Coaxial two-stage cyclone combustor (unit : mm)

Table 2 Properties of Alaska, US Coal

Proximate Analysis (Dry Air Basis):	
Volatiles	49.39%
Fixed Carbon	31.49%
Ash	8.18%
Moisture	10.05%
Ultimate Analysis:	
Carbon	68.82%
Hydrogen	6.18%
Nitrogen	1.27%
Sulphur	0.65%
Oxygen	23.08%
Calorific Value	6,050 kcal/kg
Density	1,250 kg/m^3

Table 3 Operating conditions of combustor

Pre-combustor	
Primary Air Flow	0.4 m^3/min
Secondary Air Flow	0.4 m^3/min
Primary Air Temperature	25 °C
Secondary Air Temperature	300 °C
Coal Flow	5 kg/hr
Main Combustor	
Primary Air Flow	0.2 m^3/min
Secondary Air Flow	1.03 m^3/min
Primary Air Temperature	25 °C
Secondary Air Temperature	300 °C
Coal Flow	15, 20, 25 kg/hr

is 61.4 μm. The particle size distribution is represented by a Rosin-Rammler function and discretized into ten size classes. Ten identical particles are traced from each primary port cell to take into account the adequate turbulent particle dispersion. The properties of Alaska, US coal and operating conditions are shown in Tables 2 and 3, respectively (Choi et al., 1999). Numerical simulation was performed using power-law scheme and SIMPLEC algorithm. The number of grids for the calculation domain is 119×46.

4. Results and Discussions

Figure 2 shows the calculated gas flow patterns and velocity contours near the main burner exit.

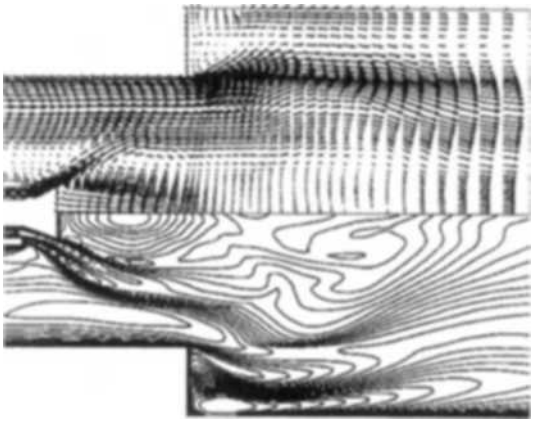

Fig. 2 Gas flow patterns and velocity contours near the main burner exit (Deflector angle=20°)

An internal recirculation flow zone is established due to the presence of the deflector. Deflector is equipped at the tip of the main burner exit and has a function of deflecting the gas and coal flow when injected to the main combustor. In this study, the deflector angle is named as an in-scattering angle and has its values of 0°, 10°, 20°, 30° and 40°. Deflected injection through main burner moves gas flows upward, and those flows are affected by the strong swirling flows in the main combustor and rotate around the wall.

Figure 3 compares the predicted and measured temperature distributions at the wall of the combustor when coal flow rates in the main combustor are varied: 15, 20, 25 kg/hr and corresponding stoichiometric air/fuel ratios are 1.13, 0.90, 0.75, respectively. The experimental results are from the study of Choi et al. (1999). The comparison shows that the general features of the temperature profiles are predicted satisfactorily for the given range of mass flow rate. While the temperature in the pre-combustor is relatively low, the supply of burned gas from the pre-combustor and heated secondary air from inlet 4 increase the temperature in the main combustor gradually. As the coal flow rate through inlet 1 increases, the wall temperature near the downstream of the combustor increases. The concept of fuel staging is characterized by the additional supply of the fuel in the main chamber, and the combustion is affected by the fuel injection in the

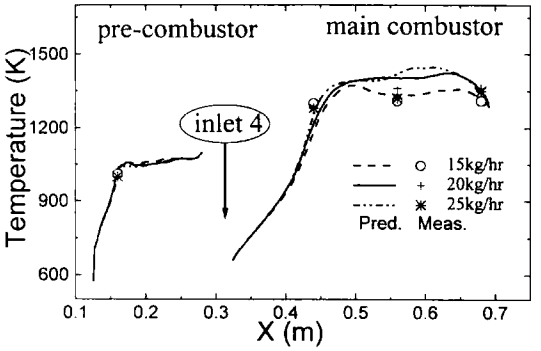

Fig. 3 Comparisons of predicted and measured wall temperature distributions for various coal mass flow rates

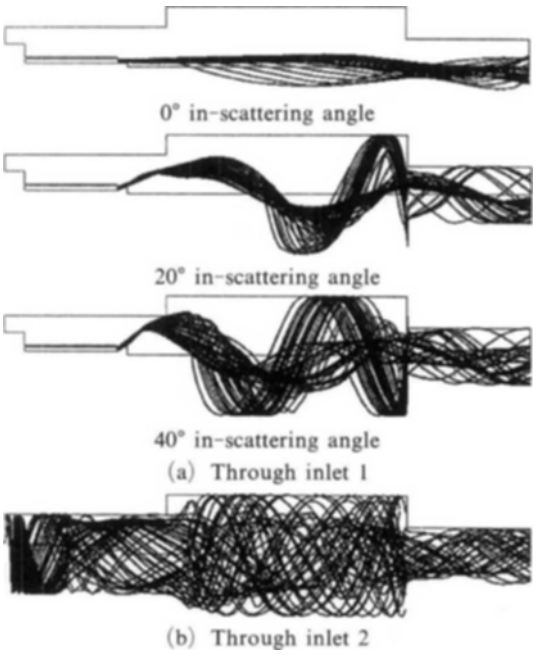

Fig. 4 Trajectories of coal particles (a) through inlet 1 for 0°, 20° and 40° in-scattering angles and (b) through inlet 2

downstream area.

Trajectories of coal particles injected through inlet 1 for in-scattering angles of 0°, 20° and 40° and inlet 2 are shown respectively in Fig. 4, and illustrate the effect of swirl on particle motions. In the case of 0° in-scattering angle, coal particles through inlet 1 fly along the axis and leave the combustor almost directly. But as the in-scattering angle increases, coal particles show

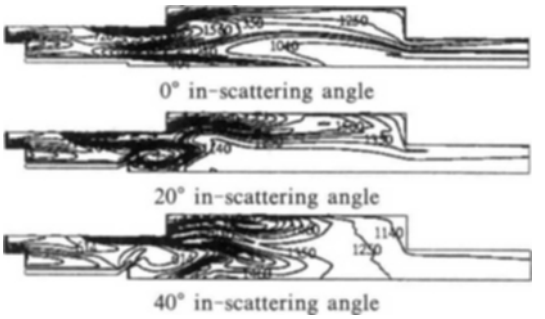

Fig. 5 Temperature contours when coal mass flow rate through inlet 1 is 20 kg/hr with 0°, 20° and 40° in-scattering angles

spiral trajectories affected by the swirling flow and have enough residence times in the main combustor so that high temperature zone along the wall is obtained. Particles through inlet 2 mostly burn in the pre-combustor with swirling flow before reaching the main combustor and supply the burned gas at high temperature to the main combustor.

Figure 5 shows the predicted temperature contours when coal mass flow rate through inlet 1 is 20 kg/hr and in-scattering angles are 0°, 20° and 40°. It shows high temperature zones in the vicinity of the walls of the pre-combustor and the main combustor. In particular, the strong influence of swirling flow in the main combustor for an 20° in-scattering angle results in a reverse flow zone near the main burner exit. It shows a similar trend with the typical burner configuration in cylindrical furnaces composed of two coaxial air streams. But particle trajectories don't show such a reverse flow. In the case of 40° in-scattering angle, coal particles seem to block the flow from the pre-combustor and deteriorate the temperature distribution, which means that the high temperature zone is confined in the upstream part of the main combustor.

Figures 6 and 7 show respectively the predicted near wall temperature distributions and the predicted radial distributions of gas temperatures at several axial stations in the main combustor when in-scattering angle varies (0°, 10°, 20°, 30°, 40°). For the complete burnout of particles, the combinations of rapid heating and long residence time are essential. Rapid heating of coal particles

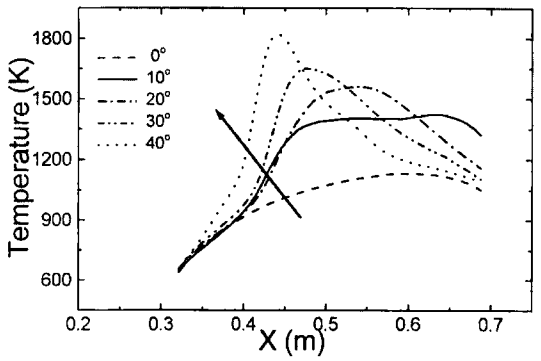

Fig. 6 Predicted near wall temperature distributions for various in-scattering angles

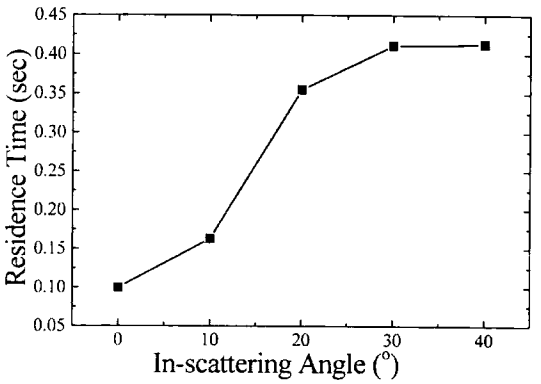

Fig. 8 Mean residence times of coal particles through inlet 1 for various in-scattering angles

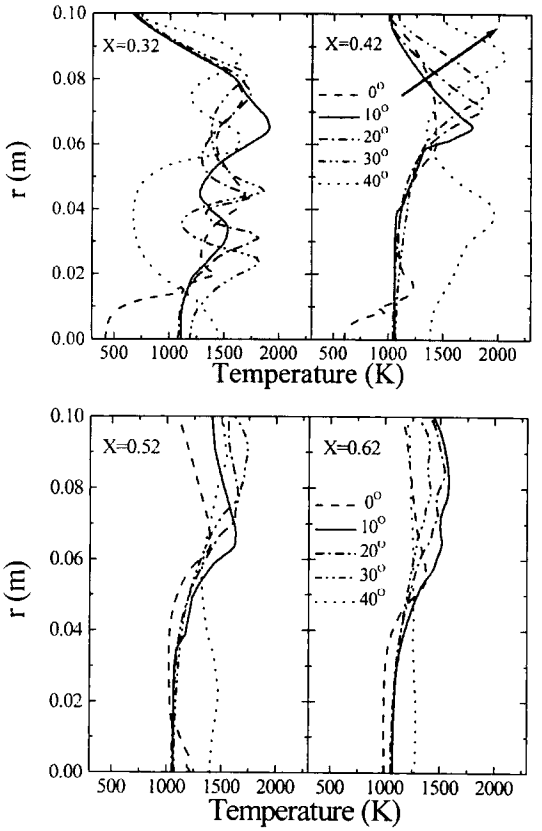

Fig. 7 Predicted radial temperature distributions at several axial stations for various in-scattering angles

through inlet 1 is affected by the burned gas from the pre-combustor and the heated air from inlet 4. If those conditions are satisfied, in-scattering angle plays an important role in the residence time of coal particles. In the case of 0° in-scattering angle, coal particles leave the combustor almost directly and show low temperature distribution along the axis, but high temperature distribution near the wall which is heated by hot gas from the pre-combustor. As the in-scattering angle increases, high temperature zone and fast burnout occur in the upper part of the main combustor and contribute to the rapidly increased temperature in the main combustor. Therefore, it is concluded that an adequate in-scattering angle is required to improve the combustion efficiency as well as to avoid slagging or fouling phenomena in the boiler which is connected to the combustor. Since the case with high in-scattering angle over 20°, however, doesn't show good effects near the main burner exit, 20° in-scattering angle would be recommended.

Figure 8 shows the mean residence times of coal particles through inlet 1 with various in-scattering angles. As in-scattering angle increases, residence times of coal particles increase due to the swirling flow, and the effect is great for large coal particles. But when the in-scattering angle is greater than 20°, mean residence time increases gradually.

In the air-staged combustion of pulverized coal, the primary air-deficient zone reduces the formation of nitrogen oxides. The complete burnout of coal particle is achieved only with the addition of secondary air. In order to understand the effects of air staging, the flow rates of

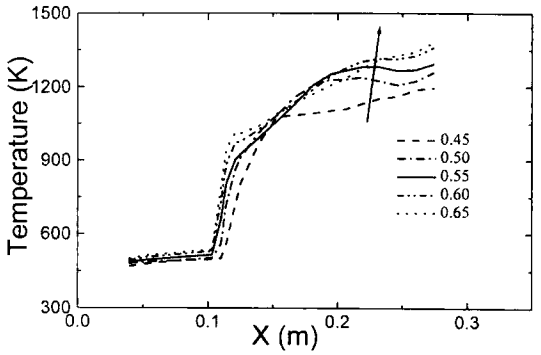

Fig. 9 The effects of secondary air on the mass weighted average temperature distribution in the pre-combustor

secondary air in the pre-combustor is varied to 0.2, 0.3, 0.4, 0.5, 0.6 m^3/min, which correspond to stoichometric air/fuel ratios of 0.45, 0.50, 0.55, 0.60, 0.65 for the coal feed rate of 20 kg/hr in the pre-combustor. As the flow rate of secondary air increases, mass weighted average temperature distributions in the pre-combustor increase as shown in Fig. 9. Even though the air flow rate varies widely, it doesn't show any unstable combustion phenomena resulting from the separate air injections.

5. Conclusions

The present study describes the coal combustion characteristics in a newly developed coaxial 2-stage cyclone combustor. As the flow rate of coal through the main burner increases, the delayed coal combustion keeps the temperature low near the burner exit, but high in the downstream of the combustor. For an air staging, as the flow rate of secondary air increases, mass weighted average temperature in the pre-combustor increases.

Coal particles through the main burner without a deflector are not easily affected by the swirling motion. Therefore, the in-scattering angle of about 20° is recommended to achieve higher combustion efficiency in this study. This condition keeps the coal particles through the main burner from leaving the combustor directly and also increases the residence time of those coal particles, resulting in a high temperature field and a rapid burnout in the main combustor.

The influence of the strong swirling flow in the main combustor for the in-scattering angle of 20° results in a reverse flow zone near the main burner exit. It shows a similar trend with the typical burner configuration in cylindrical furnaces composed of two coaxial air streams. But particle trajectories don't show such a reverse flow pattern. Predicted temperature distributions show a good agreement with corresponding experimental data.

Acknowledgment

This work was supported by the Combustion Engineering Research Center in Korea.

References

Abbas, T., Charoensuk, J., Costen, P. and Lockwood, F. C., 1997, "The Performance of Pulverized-Coal Flames in a Simulated Combined Cycle Unit," *Combustion and Flame*, Vol. 111, pp. 111~123.

Anagnostopoulos, J. S., Sargianos, N. P. and Ergeles, G., 1993, "The Prediction of Pulverized Greek Lignite Combustion in Axisymmetric Furnaces," *Combustion and Flame*, Vol. 92, pp. 209~221.

Badzioch S. and Hawksley, P. G. W., 1970, Ind. Eng. Chemical Process Des., Develop, Vol. 9, No. 4, p. 521.

Baum, M. M. and Street, P. J., 1971, "Predicting the Combustion Behavior of Coal Particles," *Combust. Sci. Tech.*, Vol. 3, pp. 231~243.

Choi, S. I., Park, C. S., Kim, S. O. and Kim H. Y., 1999, "A Study on Low Emission Pulverized Coal Combustion in the 2 Staged Coaxial Cyclone Combustor," *Journal of the Korean Society of Combustion*, Vol. 4, No. 1, pp. 67~83.

Field, M. A., 1969, "Rate of Combustion of Size-Graded Fractions of Char from a Low-Rank Coal between 1200 °K and 2000 °K," *Combustion and Flame*, Vol. 13, pp. 237~251.

Jamaluddin, A. S., Wall, T. F. and Truelove,

J. S., 1987, "Modelling of High Intensity Combustion of Pulverized Coal in a Tubular Combustor," *Combust. Sci. Tech.*, Vol. 55, pp. 89~113.

Kimoto, M., Makino, H. and Tsuji, H., 1995, "Development of New Type Pulverized Coal Burner for Low Nox and Low Unburned Carbon Combustion," *Proceedings of the 3rd international Symposium on coal combustion science and technology*, pp. 259~266.

Lockwood, F. C. and Mahmud, T., 1988, "The Prediction of Swirl Burner Pulverised Coal Flames," *Twenty-Second Symposium (International) on Combustion*, pp. 165~173.

Lockwood, F. C., Rizvi, S. M. A., Lee, G. K. and Whaley, H., 1984, "Coal Combustion Model Validation Using Cylindrical Furnace Data," *Twentieth Symposium (International) on Combustion*, pp. 513~522.

Nikjooy, M., So, R. M. C. and Peck, R. E., 1988, "Modelling of Jet-and Swirl-Stabilized Reacting Flows in Axisymmetric Combustors," *Combust. Sci. Tech.*, Vol. 58, pp. 135~153.

Shim, S. Y., Sohn, K. H. and Lee, C. S., 1994, "A Study on the Combustion Characteristics of Swirling Jet Combustor," *Transactions of the Korean Society of Mechanical Engineers*, Vol. 18, No. 2., pp. 492~501.

Spliethoff, H., Greul, U., Rudieger, H. and Hein, K. R. G., 1996, "Basic Effects on NOx Emissions in Air Staging and Burning at a Bench-Scale Test Facility," *Fuel*, Vol. 75, No. 5, pp. 560~564.

Truelove, J. S., 1984, "The Modelling of Flow and Combustion in Swirled, Pulverized-Coal Burners," *Twentieth Symposium (International) on Combustion*, pp. 523~530.

Visser, B. M., Smart, J. P., Kamp, V. D. and Weber, R., 1990, "Measurements and Predictions of Quarl Zone Properties of Swirling Pulverised Coal Flames," *Twenty-Third Symposium (International) on Combustion*, pp. 949~955.

Weber, R., Dugue, J., Sayre, A. and Visser, B. M., 1992, "Quarl Zone Flow Field and Chemistry of Swirling Pulverized Coal Flames: Measurements and Computations," *Twenty-Fourth Symposium (International) on Combustion*, pp. 1373~1380.